Carbohydrate Polymers 88 (2012) 1334–1341

Contents lists available at SciVerse ScienceDirect

Carbohydrate Polymers

journal homepage: www.elsevier.com/locate/carbpol

The effect of annealing and cryoprotectants on the properties of vacuum-freeze dried starch nanoparticles

Ai-Min Shi[a,1], Li-Jun Wang[b,1], Dong Li[a,*], Benu Adhikari[c]

[a] College of Engineering, China Agricultural University, P.O. Box 50, 17 Qinghua Donglu, Beijing 100083, China
[b] College of Food Science and Nutritional Engineering, China Agricultural University, Beijing, China
[c] School of Health Sciences, University of Ballarat, VIC 3353, Australia

ARTICLE INFO

Article history:
Received 31 December 2011
Received in revised form 28 January 2012
Accepted 7 February 2012
Available online 15 February 2012

Keywords:
Starch nanoparticles
Vacuum freeze drying
Mini-emulsion
High-pressure homogenization
Cryoprotectants
Annealing

ABSTRACT

Starch nanoparticles prepared through high pressure homogenization and mini-emulsion cross-linking technology were successfully vacuum-freeze dried. Annealing process was introduced in the drying process and the cryoprotectants (lactose and mannitol) were used in the sample matrix. The effect of the annealing and cryoprotectants on the moisture content, glass transition temperature (T_g), amorphous/crystalline nature, particle size, morphology and the redispersibility of these nanoparticles was investigated. The residual moisture content of the nanoparticles was 4–9% (w/w) and it was lower in samples which were unannealed and contained cryoprotectants. Mannitol as cryprotectant resulted into starch nanoparticles with uniform spherical shape. The T_g of these nanoparticles varied from 52 °C to 57 °C and the difference was due to annealing and cryoprotectants. The annealing process and the presence of cryoprotectant did not hugely affect the X-ray diffraction pattern and FT-IR spectra which revealed the fully cross-linked and amorphous glassy state of starch nanoparticles.

1. Introduction

Starch nanoparticles produced through nano-technological process have drawn greater attention as they are non-hazardous to human health and provide greater opportunity for mass production (Chakraborty, Sahoo, Teraoka, Miller, & Gross, 2005; Le Corre, Bras, & Dufresne, 2010). These starch nanoparticles are finding increasing application in food packaging, drug delivery and paper making (Avella et al., 2005; Simi & Emilia Abraham, 2007; Yoon & Deng, 2006).

Nanoparticles from natural materials such as starch, gelatin and chitosan can be produced using water-in-oil mini-emulsion polymerization or mini-emulsion cross-linking. One of the key steps in this technology is creation of stable mini-emulsion containing nano-sized droplets. Solans, Izquierdo, Nolla, Azemar, and Garcia-Celma (2005) and Asua (2002) reported that high speed rotary homogenization, ultrasound homogenization and high pressure homogenization are the main physical methods for preparing mini-emulsions. Considering the level of energy requirement and system stability, high pressure homogenization is more effective and promising than the other two physical methods and has proven to be better than the chemical methods in preparing stable mini-emulsions (Asua, 2002; Solans et al., 2005).

It has been reported that the drying process affects the surface morphology and internal structure of nanoparticles (Abdelwahed, Degobert, Stainmesse, & Fessi, 2006a; Lopes, Eleutério, Gonçalves, Cruz, & Almeida, 2011; Mohajel et al., 2011). Various drying methods such as spray drying, vacuum drying, freeze drying and vacuum-freeze drying are being used for drying of nanoparticles (Beirowski, Inghelbrecht, Arien, & Gieseler, 2011; Lee, Heng, Ng, Chan, & Tan, 2011; Wang et al., 2005). Among these methods, spray drying involves atomization of the feed through a nozzle or multiple nozzles and nanoparticles are formed when the droplets are dried. Vacuum drying can enhance the evaporation of water as it uses low air pressure. Freeze drying produces the nanoparticles through sublimation and particles so formed have higher porosity. Vacuum-freeze drying combines the advantage of vacuum drying and freeze drying and by doing so it can preserve the inner structure of particles at the same time enhances the rate of sublimation of water (Claussen, Ustad, Strømmen, & Walde, 2007; Ratti, 2001). Therefore, in order to better maintain the dispersibility of the nanoparticles and to avoid or minimize the generation of agglomerates, vacuum freeze drying is a good choice for preparation of nanoparticles from biological origin such as starch.

Vacuum freeze drying is a complex process because it consists of freezing component as well as vacuum drying component (Liapis & Bruttini, 1995). In vacuum freeze drying, the suspension containing nanoparticles is frozen under a low temperature to stabilize

* Corresponding author. Tel.: +86 10 62737351; fax: +86 10 62737351.
E-mail address: dongli@cau.edu.cn (D. Li).
[1] These authors contributed equally to this work.

0144-8617/$ – see front matter © 2012 Elsevier Ltd. All rights reserved.
doi:10.1016/j.carbpol.2012.02.013

or freeze the position of particles. The frozen water or solvent is removed subsequently through sublimation and nanoparticles are obtained. Simultaneous heat and mass transfer occurs in vacuum-freeze drying and various methods have been developed to enhance the heat and mass transfer rates during the drying stage (Patil, Dandekar, Patravale, & Thorat, 2010). Annealing is one of the most common and most effective methods which can increase the ice crystal size (Hottot, Vessot, & Andrieu, 2005; Patil et al., 2010). The annealing process can increase heat and mass transfer rate which is controlled by either heat transfer flux from the shelf and from the surrounding towards the ice sublimation front inside the vial or by water vapor mass transfer through the dried layer (Patil et al., 2010). Recently, many researchers have reported that annealing process enhances the drying rate during freeze drying (Abdelwahed, Degobert, & Fessi, 2006b; Lu & Pika, 2004). However, there are no publications reporting the effect of annealing on the physico-chemical characteristics of vacuum freeze dried nanoparticles.

The freezing process can also cause some damage to the nanoparticles due to freezing of water molecules within the nanoparticles. It has been reported that there is some discernible difference in the appearance and redispersibility of freeze dried particles in the presence and absence of cryoprotectants (Abdelwahed et al., 2006a; Patil et al., 2010).

Thus, in this study, we dried the starch nanoparticles produced through mini-emulsion crosslinking and high pressure homogenization using vacuum freeze drying. We also aimed at studying the effect of annealing and the presence of cryoprotectant on the physical properties of vacuum-freeze dried starch nanoparticles. The surface morphology, glass transition temperature, zeta potential, crystal structure, particle size and size distribution and moisture content were measured as physical properties of nanoparticles.

2. Materials and methods

2.1. Materials

Soluble starch, mannitol and lactose monohydrate were purchased from Beijing Aoboxing Biological Technique Company (Beijing, China) and used without further purification. Sodium chloride, sodium hydroxide, cyclohexane, acetone and acetic acid were purchased from Beijing Chemical Company (Beijing, China). Tween-80 and Span-80 were purchased from Tianjing Fuchen Chemical Company (Tianjing, China). Sodium trimetaphosphate (STMP) was obtained from Tianjing Dengfeng Chemical Company (Tianjing, China). All of these reagents were of analytical grade and used without further purification. Deionized water was used throughout the work.

2.2. Preparation of starch nanoparticles

The starch nanoparticles were produced using the emulsion cross-linking technology using a high pressure homogenizer. Starch was hydrolyzed with sodium hydroxide and then cross linked with STMP within the nanometer sized water droplets which were dispersing in oil emulsion by high speed shearing instrument (IKA® T25 digital, Staufen, Germany) at 5000 rpm for 2 min and high pressure homogenizer (ATS® AH-100D, BVI, Canada) at 30 MPa for 1 cycle. Starch nanoparticles were obtained after a series of washing steps. The details of this technology are reported elsewhere (Shi, Li, Wang, Li, & Adhikari, 2011).

2.3. Pretreatment of the sample for drying process

After washing the starch nanoparticles twice using acetone, these particles were dispersed into 100 ml deionized water. This suspension was stirred for 1 h to ascertain that all the starch nanoparticles were completely dispersed. Subsequently, the cryoprotectants were added into the suspension in appropriate proportion (mannitol, 0.2%, w/v; lactose, 0.5%, w/v). The suspension which did not contain the cryoprotectants was used as control.

2.4. Vacuum freeze drying of starch nanoparticles

A laboratory-scale vacuum freeze dryer (LGJ-18, Sihuan, China) was used to dry the suspension containing starch nanoparticles and cryoprotectants and the control. The vacuum freeze drying process consisted of the flowing two main process steps.

(1) *Freezing process*. The sample dishes containing the dispersion were placed in the cold trap of the vacuum freeze dryer. The samples were divided in Group A and Group B.
   - Group A samples (suspensions with and without cryoprotectant as described in Section 2.3) were placed in the cold traps for 7 h at −60 °C and the sample temperature changed from 15 °C to −40 °C.
   - Group B samples (suspensions with and without cryoprotectants as described in Section 2.3) were first kept in the cold traps (−60 °C) for 3 h and the temperature of sample changed from 15 °C to −30 °C. Then the sample dishes were moved into a refrigerator (−15 °C) for 2 h while the temperature of sample increased from −30 °C to −15 °C. After this annealing process, the sample dishes was shifted to cold traps (−60 °C) for 2 h and finally the sample temperature was decreased to −40 °C.

(2) *Vacuum drying process*. The dishes containing frozen suspension were then placed in drying chamber and then the chamber was evacuated. The pressure within the chamber was maintained under 100 Pa. The temperature of frozen samples was varied from −30 °C to 45 °C step by step in the 28-h-long drying period (1 h each at −30 °C, −25 °C, −20 °C, −15 °C, −10 °C, −5 °C; 2 h each at 0 °C, 5 °C, 10 °C, 15 °C, 20 °C, 25 °C, 30 °C, 35 °C, 40 °C and finally 4 h each at 40 °C and 45 °C).

2.5. Characterization of dried starch nanoparticles

2.5.1. Moisture analysis

The moisture content of each sample was determined using oven drying method as described in AOAC Method 984.25 (AOAC Official Method 984.25).

2.5.2. Appearance and morphology

The morphology of the starch nanoparticles was examined by using scanning electron microscope (SEM) (S-3400N, Hitachi, Japan). The sample was placed and dispersed on a circular platform and then plated with gold. All the samples were examined at two magnifications (10,000× and 20,000×).

2.5.3. Redispersibility, particle size and zeta potential

Redispersibility. 0.02 g dried nanoparticles sample was added into 20 ml deionized water. The time required for the redispersion of the sample and existence of visible particles was determined by gently agitating the mixture suspension (Skanderby, Westergaard, Partridge, & Muir, 2009).

Particle size and zeta potential. After stirring the nanoparticles in water for 20 min, the suspension was examined using laser particle size analyzer (Nano ZS-90, Malvern, England) for particle size and the zeta potential.

2.5.4. Glass transition temperature measurement

The glass transition temperature of dried starch nanoparticles was measured using a differential scanning calorimeter (DSC) (Q10, TA Instrument, America). Powder samples of 4–6 mg were weighed

Table 1
Effect of different cryoprotectants and annealing on the appearance, moisture content and glass transition temperature (T_g) of the vacuum-freeze dried starch nanoparticles.

Cryoprotectants[a]	Annealing treatment[b]	Appearance[c]	Moisture content (%,w/w)[d]	T_g (°C)[d]
None	+	–	8.97 ± 0.15^{e}	52.44 ± 0.05^{e}
Mannitol	+	++	7.06 ± 0.21^{f}	54.44 ± 0.13^{f}
Lactose	+	+	5.49 ± 0.10^{g}	56.56 ± 0.07^{g}
None	–	–	8.15 ± 0.02^{h}	53.59 ± 0.03^{h}
Mannitol	–	++	6.91 ± 0.14^{f}	52.11 ± 0.08^{i}
Lactose	–	+	4.51 ± 0.15^{i}	54.56 ± 0.20^{f}

[a] The optimum concentration of each cryoprotectant.
[b] +: vacuum-freeze drying with annealing; –:vacuum-freeze drying without annealing.
[c] ++: best, loose and powder; + better, fluffy and mostly powder; –: foam, fluffy but not powder; –:softy, not fluffy and rugged texture.
[d] Values of the moisture content and T_g represent the mean ± SD ($n = 3$). Values in a column followed by different lowercase letters in superscripts were significantly different from each other according to Student's t-tests ($p < 0.05$).

in aluminum pans and sealed using perforated aluminum caps. The thermal analyses were performed in two-cycle mode, covering a temperature range of −25 °C to 100 °C. A heating rate of 10 °C/min was used throughout. Nitrogen was used as flushing gas. The first heating cycle was used to remove the thermal history of the samples. The thermograms obtained from second heating cycle were used to determine the glass transition temperature (T_g) using Universal Analysis software of TA Instruments.

2.5.5. Structural analysis

Fourier-transform infrared spectroscopic (FT-IR) studies were performed in transmission mode on a Spectrum RX spectrometer (Spectrum RX/BX series, Perkin Elmer, USA). The FTIR spectra of the dried starch nanoparticles were compared with that of the native soluble starch (raw material, Section 2.1). Tablets comprising 300 mg of KBr and 2 mg of starch nanoparticles were prepared for FTIR tests. Spectra were obtained at 4 cm^{-1} of resolution from 4000 cm^{-1} to 400 cm^{-1}. The interference of water and CO_2 from air was deducted during scanning.

X-ray diffraction patterns of the dried starch nanoparticles, native soluble starch, NaOH, STMP, NaCl, mannitol and lactose were recorded at room temperature using an X-ray diffractometer (XD-2, PuXiTongYong, China). The slit width of 1° and the 2θ range from 5° to 45° in steps of 0.02° per 1 s were used. All the samples were compacted to form an even surface.

2.6. Statistical analysis

All the experiments were carried out in triplicate and the level of (significance) difference was analyzed using Duncan's multiple range tests at 0.95 confidence level.

3. Results and discussion

3.1. Preparation of starch nanoparticles

Due to the cross-linking reaction between starch and Sodium trimetaphosphate (STMP) (Shi et al., 2011), starch nanoparticles were first solidified as spherical particles within the droplets of mini-emulsion. As reported in our previous research (Shi et al., 2011), the particle size of starch nanoparticles in the w/o emulsion was varied from 354.6 nm to 135.9 nm when the homogenization pressure was varied from 10 MPa to 50 MPa. In this study, the average size of starch nanoparticles in the solution was found to be 378 ± 14 nm which is slightly larger than that in the w/o emulsion most probably due to swelling in aqueous medium.

3.2. Moisture analysis

The moisture content values of dried starch nanoparticles are presented in Table 1. The moisture content values of the particles obtained from different annealing protocol and having the presence of cryoprotectants are listed in this table. It can be seen from this table that the particles obtained in the presence of cryoprotectants have generally lower moisture content than the particles obtained without the use of the cryoprotectants. It can also be observed from Table 1 that the moisture content values of the particles obtained after the annealing treatment (during freezing) are slightly higher than the moisture content values of the particles which were not subjected to annealing treatment. For example, the starch nanoparticles obtained using lactose as cryoprotectant and when the annealing treatment was not carried have the lowest moisture content of 4.51 ± 0.15% (w/w). It can also be observed from this table that the starch nanoparticles obtained without using cryoprotectant but were subjected to annealing process have the highest moisture content of 8.97 ± 0.15% (w/w).

Cryoprotectants such as mannitol and lactose are commonly used to protect sensitive biological specimens from freezing related damage or injury. It is generally accepted that the cryoprotectants form hydrogen bonds with biological molecules *in lieu* of water molecules when water molecules are displaced. Thus, as the cryoprotectant replaces the water molecules during freezing stage most ice crystals can be insulated by these cryoprotectants. In this way the chilling or freezing injury in sensitive materials such as starch nanoparticles can be greatly minimized (Patil et al., 2010). At the same time, when the molecules of cryoprotectants preferentially interact or hydrogen-bond with the starch nanoparticles, this frees more water molecules to evaporate to drying air ultimately resulting into lower moisture content in dried starch nanoparticles.

When freezing temperatures are lower than −60 °C, the entire water molecules in the sample get solidified into ice crystals and the differences in the samples with and without annealing get reflected in the particle size and the distribution of ice crystals. Even though the annealing process can enhance the sublimation rate of ice crystals, it still can give rise to many other defects. For example, larger ice crystal can affect the sublimation of ice crystal as thermal energy required for sublimation cannot easily penetrate to the interior of the sample (Patil et al., 2010). All these drawbacks affect the rate of sublimation in the sample which ultimately results into different residual moisture contents.

3.3. Morphological analysis

The appearance of dried starch nanoparticles is presented in Fig. 1 and summarized in Table 1. The samples having mannitol as cryoprotectant had more porous and loose or fluffy morphology whether the sample was annealed or not. The nanoparticles produced using mannitol as cryoprotectant had more appealing morphology compared to that of the other two: the sample without cryoprotectant and the one with lactose as cryoprotectant. It may be due to the fact that the mannitol can decrease the rate of formation

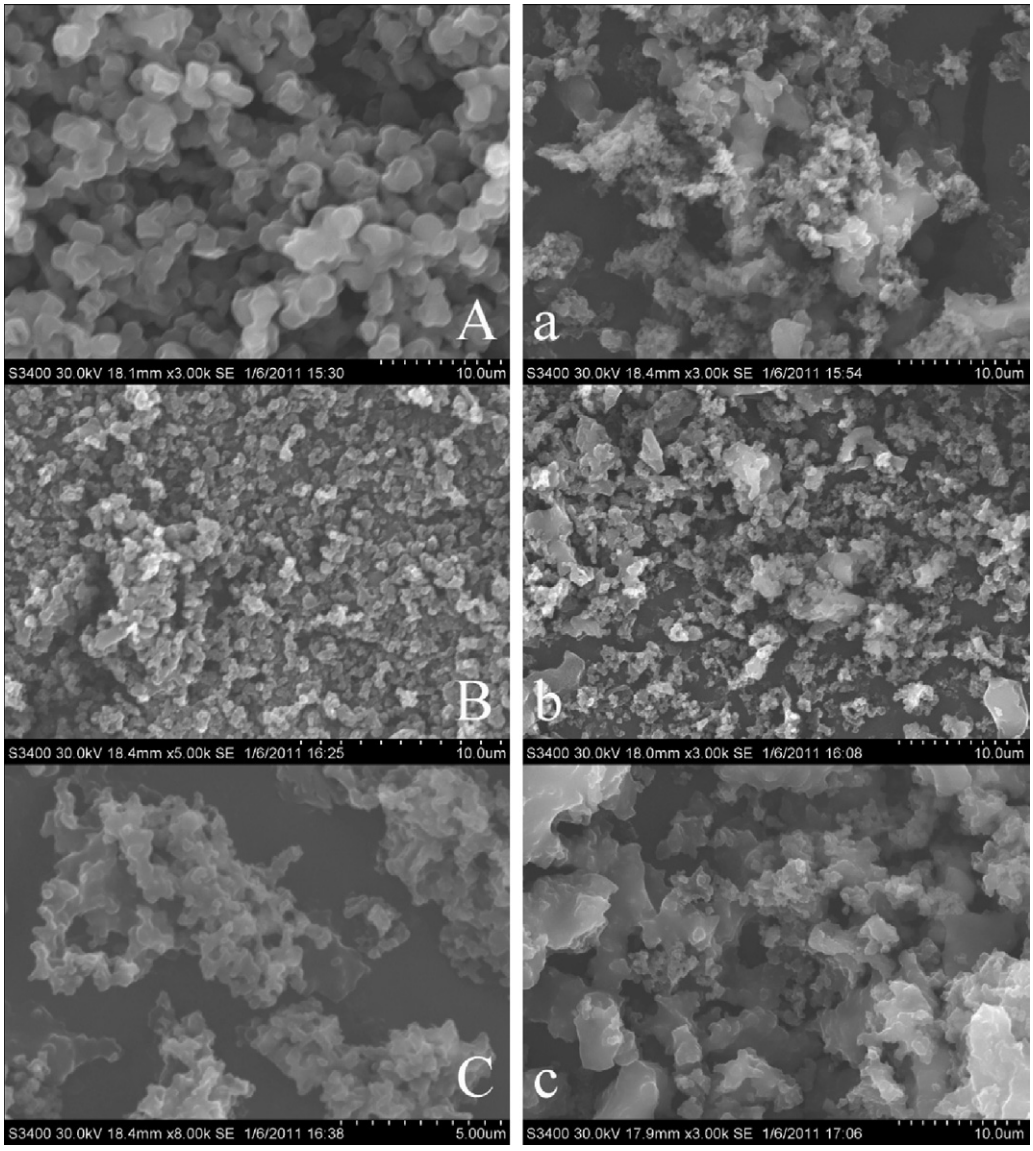

Fig. 1. The scanning electron micrographs of dried starch nanoparticles: A, B and C represent sample without annealing; a, b, and c with annealing; A and a represent sample without any cryoprotectant; B and b represent sample with mannitol as cryoprotectant; C and c, represent sample with lactose as cryoprotectant.

of ice crystals in the interior and in the exterior bulk of the starch nanoparticles. This means that the starch nanoparticles can get surrounded by ice crystals when mannitol is used as cryoprotectant. Whereas, when lactose is used as cryoprotectant, it forms a stable amorphous/glassy protective matrix around the starch nanoparticles. This kind of protective matrix can reduce the damage of ice crystal to starch nanoparticle which ultimately results into foam like loose morphology. However, considering the molecular structure and size, mannitol had less effect on the appearance of dried sample than lactose. Similar results were observed by Patil et al. (2010) and Barresi, Ghio, Fissore, and Pisano (2009).

Fig. 1 shows the SEM micrographs of dried starch nanoparticles under different drying condition. The left column with capital letters shows the SEM micrographs of starch nanoparticles obtained without annealing. The right column with the small letters is the SEM micrographs of starch nanoparticles which were produced by carrying out annealing.

When cryoprotectant is added in the sample during freezing/freeze drying process of starch nanoparticles, it can minimize the damage caused by ice crystal to starch nanoparticles due to former's sharp edge. Meanwhile, the annealing process can also result into different size and size distribution of the ice crystals.

As can be seen from Fig. 1, the starch nanoparticles appear to be spherical or like spheroid in all the samples. In the samples in which cryoprotectants were not added (A and a in Fig. 1), the non-annealed starch nanoparticles produced more discrete, unfused and spherical particles than those samples which were annealed. Similarly, more intact and spherical nanoparticles were obtained in samples in which cryoprotectants (mannitol and lactose) were used but were not subjected to annealing. The annealing process not only found to increase the particle size and size distribution of ice crystals but also facilitate the freezing of water molecules within the nanoparticles into ice crystals. Due to volume expansion when water solidified into ice, starch nanoparticles were found to be partly damaged by these ice crystals. This resulted into many fragments of starch nanoparticles which can be seen in the right column of Fig. 1.

The samples which did not contain any cryoprotectant produced nanoparticles with much different particle size and morphology than the samples which contained mannitol and lactose as

Table 2
Effect of different cryoprotectants and annealing process on the redispersion time, particle size and zeta potential of vacuum-freeze dried starch nanoparticles.

Cryoprotectants[a]	Annealing treatment[b]	Appearance after redispersion[c]	Redispersion time[d] (s)	Particle size[e] (*d* nm)	Zeta potential[e] (mV)
None	+	*	<170	900.13 ± 83.43[f]	−25.00 ± 1.51[f]
Mannitol	+	**	<130	542.05 ± 16.09[g]	−32.87 ± 0.86[g]
Lactose	+	***	<60	401.87 ± 20.53[h]	−35.70 ± 0.46[h]
None	–	*	<210	796.73 ± 84.42[i]	−28.27 ± 1.69[i]
Mannitol	–	**	<170	575.85 ± 40.14[j]	−29.93 ± 1.80[j]
Lactose	–	***	<70	345.15 ± 9.43[k]	−31.19 ± 0.67[k]

[a] The optimum concentration of each cryoprotectant.
[b] +: vacuum-freeze drying with annealing; –:vacuum-freeze drying without annealing.
[c] ***: transparent or clear, rapidly redispersing; **:transparent slightly turbid; *turbid and similar to the original sample.
[d] Seconds required for redispersion with manual shaking.
[e] Values of the moisture content represent the mean ± SD ($n \geq 3$). Values in a column followed by different lowercase letters in superscripts were significantly different from each other according to Student's *t*-tests ($p < 0.05$).

cryoprotectants (Fig. 1). As we can see from the left column of Fig. 1, starch nanoparticles without any cryoprotectant were typically larger than the other two samples. For example, the particle size of starch nanoparticles with mannitol and lactose as cryoprotectant was about 500 nm while the particle size of sample without any cryoprotectant was about 1000 nm. The samples with mannitol as cryoprotectant had the best morphology in terms of size and dispersibility. On the other hand, the samples with lactose as cryoprotectant were much more agglomerated compared to the other two samples. The samples presented in both the right and left columns (Fig. 1) had similar features regarding the particle size. The morphology of these three samples presented in right column show aggregation of particles similar to those observed in particles when lactose is used as cryoprotectant (left column in Fig. 1).

Different cryoprotectants can bring about different trends in volume change during freezing process. This means that the samples containing different cryoprotectants can have different volumetric expansion coefficient when water freezes into ice. This may be the main reason why the mannitol and lactose have given rise to different particle size and morphology in the starch nanoparticles. For example, mannitol can form crystalline domains around the surface of starch nanoparticles to enhance the plasticity of starch nanoparticles whereas lactose can only maintain the amorphous state same as that of starch nanoparticles. On the other hand, the sample which does not contain any cryoprotectant does not have such protection and that the unrestricted volumetric expansion of water in the freezing process can lead to larger crystals both inside and surrounding the starch nanoparticle (Hawe & Frieß, 2006).

3.4. Redispersibility of nanoparticles

The redispersion characteristic of dried starch nanoparticles is presented in Table 2. The time required for redispersion and appearance of the suspension are used as two key indices of redispersion. As can be seen from Table 2, the sample with lactose as cryoprotectant had shorter redispersion time (<70 s) than other two dried starch nanoparticles, sample without any cryoprotectant (<210 s) and sample with mannitol as cryoprotectant (<170 s). The data presented in this table also show that the redispersion time of samples subjected to annealing process was always shorter than that of unannealed samples. In addition, the appearance of nanoparticles, especially those containing cryoprotectant, before and after dispersion was quite different. The appearance of samples without any cryoprotectant was turbid/opaque similar to the original samples. The sample with mannitol as cryoprotectant was transparent with some turbidity or opaque appearance. The sample with lactose as cryoprotectant was transparent or clear and showed greater light transmitting characteristics compared to the sample before redispersion.

The reason for the above listed differences in redispersing time and appearance of the suspension may be due to the fact that the cryoprotectants can enlarge the space between the dried starch nanoparticles and water can easily diffuse or penetrate into the interior of those nanoparticles. The annealing process can also alter the proximity of starch nanoparticles because of the formation of larger ice crystals. Hence, both the presence of cryoprotectants and the annealing process (duration and temperature of annealing) affect the redispersion time. Yet another important aspect is that the cryoprotectants can form a layer on the surface of starch nanoparticles which also facilitates the redispersion of the starch nanoparticles (Patil et al., 2010). Because of their high solubility in water, cryoprotectants can help to enhance the dispersibility of the nanoparticles which can be seen from the appearance.

3.5. Particle size and zeta potential

Table 2 also shows the particle size and zeta potential values of rehydrated starch nanoparticles in water medium. The data presented in this table show that the use of different type of cryoprotectant and annealing treatment can bring about remarkable difference in particle size and zeta potential in the dispersion. For example, the particle size of the annealed sample reduced from 900.13 ± 83.43 nm (without any cryoprotectant) to 401.87 ± 20.53 nm (with lactose as cryoprotectant). The unannealed samples also exhibited similar variation in particle size due to the presence of cryoprotectants. For example, the particle size decreased from 796.73 ± 84.42 nm (in the absence of cryoprotectant) to 345.15 ± 9.43 nm (in the presence of lactose as cryoprotectant). In addition, for a given cryoprotectant (lactose or mannitol), particle size of annealed sample was always lager than that of the annealed sample.

The reason for the differences in particle size in these suspensions may be due to the fact that the cryoprotectant can form a layer on the surface of starch nanoparticles. As the cryoprotectant layer promptly dissolves in water, it facilitates the dissolution of the starch nanoparticles in water. The fact that the lactose has a smaller molecular size than mannitol can affect not only the structure of the starch nanoparticles but also the rate of the redispersion in water. This might be one of the reasons why the starch nanoparticles with lactose as cryoprotectant have smaller particle size than those samples with mannitol as cryoprotectant. On the other hand, the starch nanoparticles pressurized by the lager ice crystals (produced during the annealing process) tend to agglomerate which can influence the measurement of particle size. As the starch nanoparticles undergo swelling the particle size of the rehydrated particles will be probably much larger than the size of starch nanoparticles before drying.

From Table 2, the absolute zeta potential of sample with lactose as cryoprotectant (35.70 ± 0.46 mV with annealing,

31.19 ± 0.67 mV without annealing) was higher than the zeta potential values in samples without any cryoprotectant (25.00 ± 1.51 mV with annealing, 28.27 ± 1.69 mV without annealing). Similarly, the zeta potential values of samples with mannitol as cryoprotectant (32.87 ± 0.86 mV with annealing, 29.93 ± 1.80 mV without annealing) were larger than the zeta potential values of samples having no protectants. Starch nanoparticles show negative surface charge because the hydrogen ions of hydroxyl groups will be exposed from starch nanoparticles. In addition, the variation in the zeta potential values might also be due to variation in the particle size and the type of cryoprotectant used (Liu, Wu, Chen, & Chang, 2009).

3.6. The glass transition temperature (T_g) of samples

The glass transition temperature (T_g) values of dried starch nanoparticles are listed in Table 1. As can be seen from this table, both the annealing process and the different cryoprotectants have affected the T_g values of the starch nanoparticles. For example, the sample with lactose as cryoprotectant had higher T_g values (56.56 ± 0.07 °C with annealing, 54.56 ± 0.20 °C without annealing) than the other samples whether or not those samples were annealed. The samples with mannitol as cryoprotectant had T_g values of 54.44 ± 0.13 °C and 52.11 ± 0.08 °C with and without annealing, respectively. However, the T_g value of starch

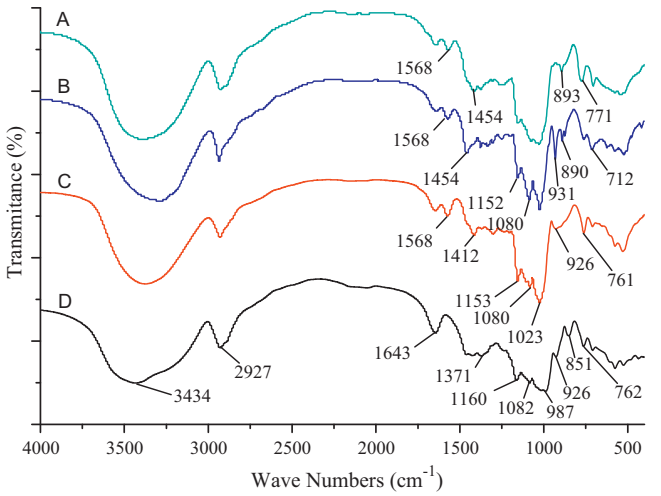

Fig. 2. FT-IR spectrum of dried starch nanoparticles: (A) represents sample with 2%(w/v) lactose as the cryoprotectant; (B) represents sample with 0.5%(w/v) mannitol as the cryoprotectant; (C) represents sample without any cryoprotectant; (D) represents soluble starch.

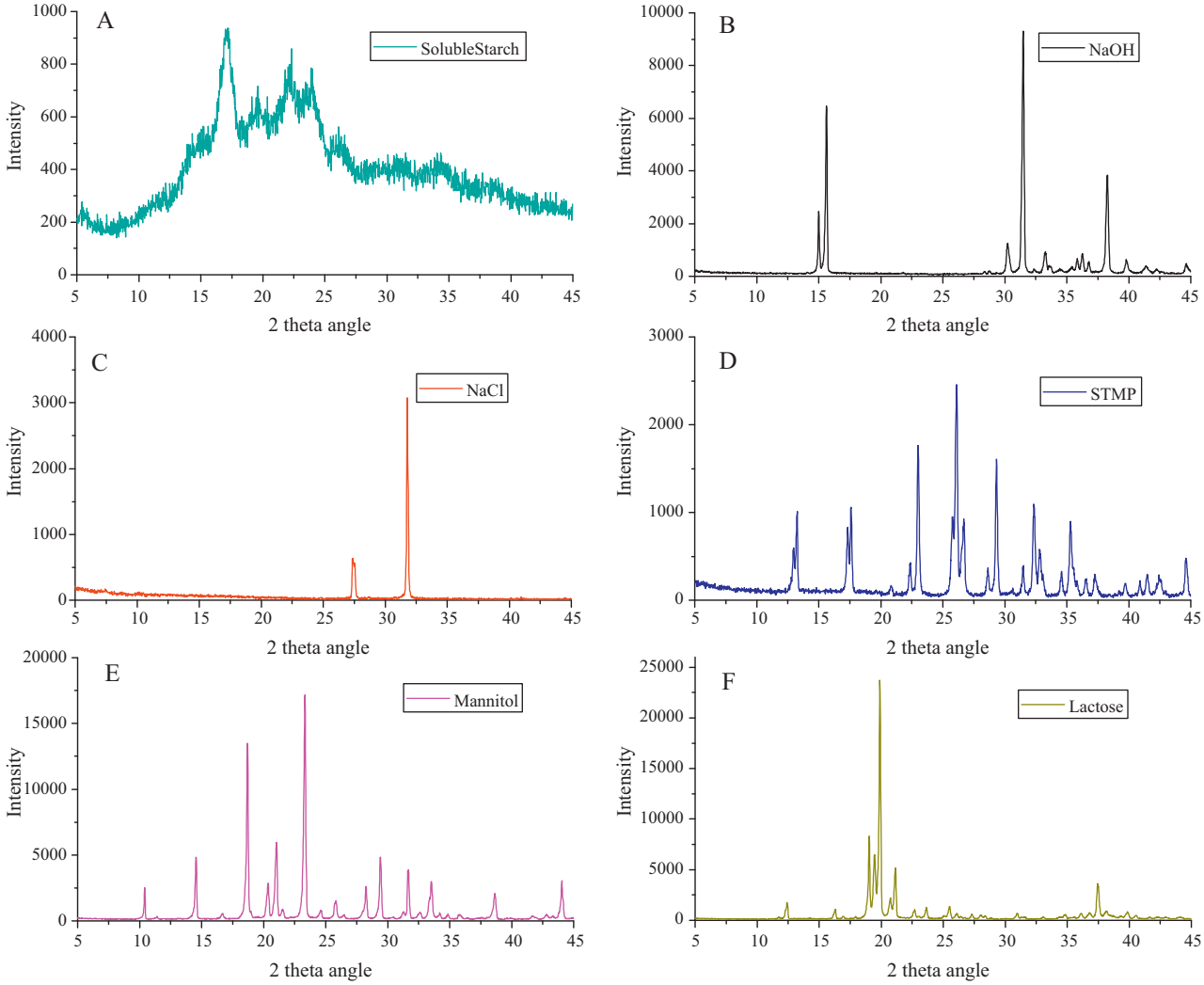

Fig. 3. XRD spectra of various components in the starch nanoparticles during vacuum-freeze drying process: (A) soluble starch; (B) NaOH; (C) NaCl; (D) sodium trimetaphosphate (STMP); (E) mannitol; (F) lactose.

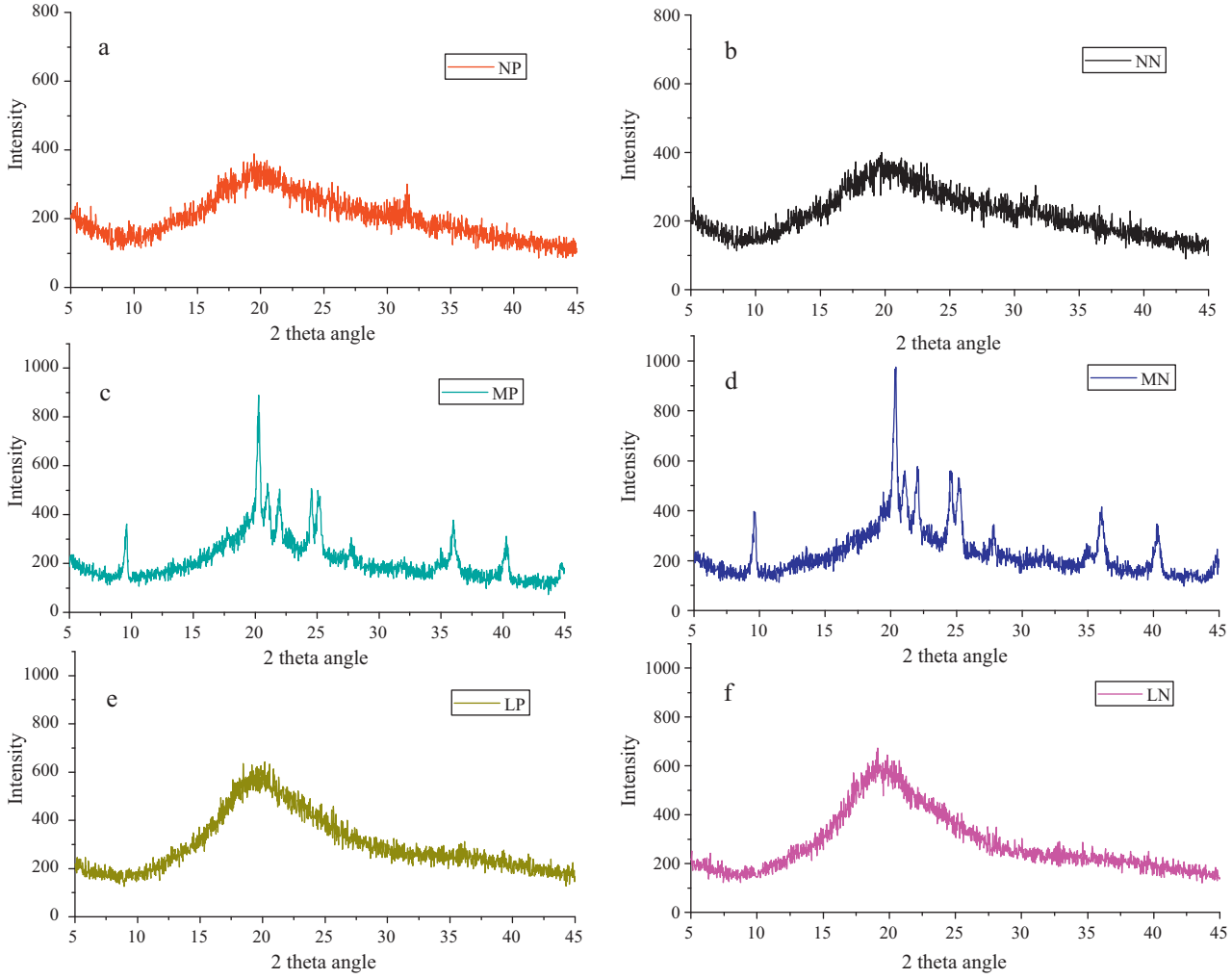

Fig. 4. XRD pattern of the vacuum-freeze dried product: (a) without any cryoprotectant, with annealing; (b) without any cryoprotectant and annealing; (c) with mannitol as the cryoprotectant, with annealing; (d) with mannitol as the cryoprotectant, without annealing; (e) with lactose as the cryoprotectant, with annealing; (f) with lactose as the cryoprotectant, without annealing.

nanoparticles which contained no cryoprotectants was $52.44 \pm 0.05\,^{\circ}C$ when it was subjected to annealing process, while it was $53.59 \pm 0.03\,^{\circ}C$ when the sample was not subjected to the annealing process.

The main reason in the variation in T_g values in the above samples is the difference in residual moisture content in the samples. As the presence of cryoprotectants having different T_g and annealing process both are capable of affecting T_g, the variation in above T_g values in these starch nanoparticle samples has followed an expected trend. As water is very strong plasticizer of starch material, the lower T_g values in samples having higher moisture contents are quite expected (Zeleznak & Hoseney, 1987).

3.7. Analysis of the physical structure

3.7.1. FT-IR spectroscopy

The FT-IR spectra of the dried starch nanoparticles are presented in Fig. 2. In this figure, the spectrum A represents sample with 2% (w/v) lactose as the cryoprotectant, spectrum B represents sample with 0.5%(w/v) mannitol as the cryoprotectant. Similarly, the spectrum C represents the sample without any cryoprotectant and spectrum D presents soluble starch. The strong absorption band at 3434 cm^{-1} is attributed to the O—H stretching of starch and its width indicates the extent of formation of inter- and intra-molecular hydrogen bonds. The asymmetric stretching of C—H (CH_2 group) is observed at 2927 cm^{-1} and the absorption band at 1643 cm^{-1} is attributed to tightly bound water present in the starch (Van Soest, Tournois, De Wit, & Vliegenthart, 1995).

Other peaks, at 1160 cm^{-1} and 1082 cm^{-1} are resulted from C—O bond and C—C bond, the peak at 1371 cm^{-1} represents the angular deformation of C—H (CH_3 group). Similarly the peak at 987 cm^{-1} is resulted from the skeletal vibration of α-1-4 glycosidic linkage (C—O—C). The peak at 762 cm^{-1} is attributed to the C—C stretching and it reflects the unique properties of soluble starch. In addition to the characteristic absorption bands of soluble starch, the dried starch nanoparticles sample (spectra A, B and C) show a series of common spectra at 1568 cm^{-1} and 1412 cm^{-1}, which are attributed to antisymmetric stretching of COO^- carboxylate radical and symmetrical stretching of COO^- group. The appearance of carboxylate radical and COO^- could be the result of the opening up of starch chains by alkali. The other peaks at 1153 cm^{-1}, 1080 cm^{-1} and 1023 cm^{-1} are resulted from the P=O, C—O—P, and O—P—O of the phosphate group, respectively. These later peaks can considered as an evidence of cross-linking between starch molecular and sodium trimetaphosphate (Xie & Shao, 2009).

The absorption peaks in the spectra of these three dried starch nanoparticles (spectra A, B and C) also show some differences which reflect the existence of cryoprotectants. Specifically, the peaks at 771 cm^{-1} and 712 cm^{-1} are strengthened due to the presence of cryoprotectants having C—OH in their molecules. On spectrum B

the peak at 1454 cm^{-1} is resulted from the COOH of mannitol (Zajc, Obreza, Bele, & Src ic, 2005).

3.7.2. X-ray diffraction patters

The X-ray diffraction patterns of dried starch nanoparticles and the raw materials involved in preparation and freeze drying process (soluble starch, NaOH, NaCl, SMTP, Mannitol, Lactose) are shown in Figs. 3 and 4. When the diffraction patters presented in the left column of Fig. 4 are compared with the diffraction patters in the right column of the same figure, it can be seen that there is no perceivable difference between the annealed and unannealed starch nanoparticles. When the diffraction pattern of soluble starch presented in Fig. 3 is compared to the diffraction patterns of the crosslinked and freeze dried nanoparticles presented in Fig. 4, one can see that the patterns show predominantly amorphous nature in latter because of the cross-linking reaction amongst the starch molecules (Shi et al., 2011), NaOH and STMP. This is also the reason why the characteristic peaks of NaCl and other cryoprotectants are observed in the diffraction patterns of dried starch nanoparticles.

The characteristic peaks observed in samples with mannitol and lactose as cryoprotectant are not the simple integration or combination of peaks occurring in the patterns of the starch nanoparticles and these cryoprotectants. These peaks are the manifestation of formation of hydrogen bonds between the molecules of starch nanoparticles and cryoprotectants.

4. Conclusions

Starch nanoparticles prepared through the combination of high pressure homogenization and w/o emulsion cross-linking technique were successfully freeze dried using vacuum-freeze dryer. Most of the starch nanoparticles were like-spheres and could be easily dispersed in w/o emulsion and water. The diameter of these nanoparticles was 263 ± 3 nm and 378 ± 14 nm in w/o emulsion and in water, respectively. The freeze dried starch nanoparticles fairly easily redissolved in water and appeared to be turbid and opaque similar to their appearance in original sample.

We found that the annealing process and the presence of cryoprotectants facilitate the formation of ice crystals both inside and around the starch nanoparticles. The morphology of starch nanoparticles and the form and size of crystals were found to be affected by the annealing process. The residual moisture content, particle size and glass transition temperature of the starch nanoparticles were found to be significantly ($p < 0.05$) affected by the annealing process and the presence of different cryoprotectants. However, chemical properties, as shown in FT-IR spectra, were not affected by the annealing process but slightly affected by the presence of cryoprotectants.

Acknowledgments

This research was supported by National Natural Science Foundation of China (30800662, 31000813), High Technology Research and Development Program of China (2011AA100802), Program for New Century Excellent Talents in University of China (NCET-08-0537), Science and Technology Support Project of China (2009BADA0B03), and Commonweal Guild Agricultural Scientific Research Project of China (201003077).

References

Abdelwahed, W., Degobert, G., Stainmesse, S., & Fessi, H. (2006). Freeze-drying of nanoparticles: Formulation, process and storage considerations. *Advanced Drug Delivery Reviews*, *58*(15), 1688–1713.

Abdelwahed, W., Degobert, G., & Fessi, H. (2006). A pilot study of freeze drying of poly(epsilon-caprolactone) nanocapsules stabilized by poly(vinyl alcohol): Formulation and process optimization. *International Journal of Pharmaceutics*, *309*(1–2), 178–188.

Asua, J. M. (2002). Miniemulsion polymerization. *Progress in Polymer Science (Oxford)*, *27*(7), 1283–1346.

Avella, M., De Vlieger, J. J., Errico, M. E., Fischer, S., Vacca, P., & Volpe, M. G. (2005). Biodegradable starch/clay nanocomposite films for food packaging applications. *Food Chemistry*, *93*, 467–474.

Barresi, A., Ghio, S., Fissore, D., & Pisano, R. (2009). Freeze drying of pharmaceutical excipients close to collapse temperature: Influence of the process conditions on process time and product quality. *Drying Technology*, *27*(6), 805–816.

Beirowski, J., Inghelbrecht, S., Arien, A., & Gieseler, H. (2011). Freeze-drying of nanosuspensions, 1: Freezing rate versus formulation design as critical factors to preserve the original particle size distribution. *Journal of Pharmaceutical Sciences*, *100*(5), 1958–1968.

Chakraborty, S., Sahoo, B., Teraoka, I., Miller, L. M., & Gross, R. A. (2005). Enzyme-catalyzed regioselective modification of starch nanoparticles. *Macromolecules*, *38*(1), 61–68.

Claussen, I. C., Ustad, T. S., Strømmen, I., & Walde, P. M. (2007). Atmospheric freeze drying—A review. *Drying Technology*, *25*(6), 947–957.

Hawe, A., & Frieß, W. (2006). Impact of freezing procedure and annealing on the physico-chemical properties and the formation of mannitol hydrate in mannitol-sucrose-NaCl formulations. *European Journal of Pharmaceutics and Biopharmaceutics*, *64*(3), 316–325.

Hottot, A., Vessot, S., & Andrieu, J. (2005). Determination of mass and heat transfer parameters during freeze-drying cycles of pharmaceutical products. *PDA Journal of Pharmaceutical Science and Technology*, *59*(2), 138–153.

Le Corre, D., Bras, J., & Dufresne, A. (2010). Starch nanoparticles: A review. *Biomacromolecules*, *11*(5), 1139–1153.

Lee, S.-H., Heng, D., Ng, W.-K., Chan, H.-K., & Tan, R. B. H. (2011). Nano spray drying: A novel method for preparing protein nanoparticles for protein therapy. *International Journal of Pharmaceutics*, *403*(1-2), 192–200.

Liapis, A. I., & Bruttini, R. (1995). Freeze drying. In A. S. Mujumdar (Ed.), *Handbook of industrial drying*. New York: Marcel Dekker.

Liu, D., Wu, Q., Chen, H., & Chang, P. R. (2009). Transitional properties of starch colloid with particle size reduction from micro- to nanometer. *Journal of Colloid and Interface Science*, *339*(1), 117–124.

Lopes, R., Eleutério, C. V., Gonçalves, L. M. D., Cruz, M. E. M., & Almeida, A. J. (2011). Lipid nanoparticles containing oryzalin for the treatment of leishmaniasis. *European Journal of Pharmaceutical Sciences*, doi:10.1016/j.ejps.2011.09.017

Lu, X-. F., & Pika, M. J. (2004). Freeze-drying of mannitol–trehalose–sodium chloride-based formulations: The impact of annealing on dry layer resistance to mass transfer and cake structure. *Pharmaceutical Development and Technology*, *9*(1), 85–95.

Mohajel, N., Roholamini Najafabadi, A., Azadmanesh, K., Vatanara, A., Moazeni, E., Rahimi, A., et al. (2011). Optimization of a spray drying process to prepare dry powder microparticles containing plasmid nanocomplex. *International Journal of Pharmaceutics*, doi:10.1016/j.ijpharm.2011.11.014

Patil, V. V., Dandekar, P. P., Patravale, V. B., & Thorat, B. N. (2010). Freeze drying: Potential for powdered nanoparticulate product. *Drying Technology*, *28*(5), 624–635.

Ratti, C. (2001). Hot air and freeze-drying of high-value foods: A review. *Journal of Food Engineering*, *49*(4), 311–319.

Shi, A.-M., Li, D., Wang, L.-J., Li, B.-Z., & Adhikari, B. (2011). Preparation of starch-based nanoparticles through high-pressure homogenization and miniemulsion cross-linking: Influence of various process parameters on particle size and stability. *Carbohydrate Polymers*, *83*(4), 1604–1610.

Simi, C. K., & Emilia Abraham, T. (2007). Hydrophobic grafted and cross-linked starch nanoparticles for drug delivery. *Bioprocess and Biosystems Engineering*, *30*(3), 173–180.

Skanderby, M., Westergaard, V., Partridge, A., & Muir, D. D. (2009). Chapter 5 Dried milk products. In *Dairy powders and concentrated products* (1st ed.). Hoboken: Blackwell Publishing Ltd., p. 231.

Solans, C., Izquierdo, P., Nolla, J., Azemar, N., & Garcia-Celma, M. J. (2005). Nano-emulsions. *Current Opinion in Colloid and Interface Science*, *10*(3-4), 102–110.

Van Soest, J. J. G., Tournois, H., De Wit, D., & Vliegenthart, J. F. G. (1995). Short-range structure in (partially) crystalline potato starch determined with attenuated total reflectance Fourier-transform IR spectroscopy. *Carbohydrate Research*, *279*, 201–214.

Wang, B., Zhang, W., Zhang, W., Mujumdar, A. S., & Huang, L. (2005). Progress in drying technology for nanomaterials. *Drying Technology*, *23*(1-2 SPEC. ISS), 7–32.

Xie, W., & Shao, L. (2009). Phosphorylation of corn starch in an ionic liquid. *Starch/Staerke*, *61*(12), 702–708.

Yoon, S., & Deng, Y. (2006). Clay–starch composites and their application in papermaking. *Journal of Applied Polymer Science*, *100*(2), 1032–1038.

Zajc, N., Obreza, A., Bele, M., & Src ic, S. (2005). Physical properties and dissolution behaviour of nifedipine/mannitol solid dispersions prepared by hot melt method. *International Journal of Pharmaceutics*, *291*(1-2), 51–58.

Zeleznak, K. J., & Hoseney, R. C. (1987). The glass transition in starch. *Cereal Chemistry*, *64*, 121–124.